NASA TECHNICAL NOTE

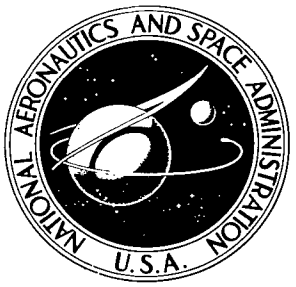

NASA TN D-5546

RADIOFREQUENCY SYSTEM ANALYSIS OF THE LEWIS CYCLOTRON MODIFICATION

by Theodore E. Fessler

Lewis Research Center

Cleveland, Ohio

NATIONAL AERONAUTICS AND SPACE ADMINISTRATION • WASHINGTON, D. C. • DECEMBER 1969

1. Report No. NASA TN D-5546	2. Government Accession No.	3. Recipient's Catalo
4. Title and Subtitle RADIOFREQUENCY SYSTEM ANALYSIS OF THE LEWIS CYCLOTRON MODIFICATION		5. Report Date December 1969 6. Performing Organization Code
7. Author(s) Theodore E. Fessler		8. Performing Organization Report No. E-5101
9. Performing Organization Name and Address Lewis Research Center National Aeronautics and Space Administration Cleveland, Ohio 44135		10. Work Unit No. 129-02 11. Contract or Grant No.
12. Sponsoring Agency Name and Address National Aeronautics and Space Administration Washington, D.C. 20546		13. Type of Report and Period Covered Technical Note 14. Sponsoring Agency Code

15. Supplementary Notes

16. Abstract

The resonant cavity of the modified Lewis Research Center cyclotron is analyzed. The results include the variation of resonant frequency with tuning panel position, an estimate of the skin resistance losses, the distribution of voltage along the length of the dee electrode, and a lumped-impedance equivalent circuit. Dee-to-dee coupling is analyzed for its influence on servotuning of the dees. A tuning function is presented which should make stable servotuning possible for any amount of dee-to-dee coupling. The performance of a shortened coupling line between the power amplifier and the dee stem is also analyzed.

17. Key Words *(Suggested by Author(s))* Cyclotron Radiofrequency system	18. Distribution Statement Unclassified - unlimited		
19. Security Classif. (of this report) Unclassified	20. Security Classif. (of this page) Unclassified	21. No. of Pages 29	22. Price * $3.00

*For sale by the Clearinghouse for Federal Scientific and Technical Information
Springfield, Virginia 22151

RADIOFREQUENCY SYSTEM ANALYSIS OF THE LEWIS CYCLOTRON MODIFICATION

by Theodore E. Fessler

Lewis Research Center

SUMMARY

The resonant cavity of the modified Lewis Research Center cyclotron has been analyzed by means of a digital computer code. In this analysis, electrical properties of the resonant cavity were obtained from its physical dimensions. The results include the variation of resonant frequency with tuning panel position, an estimate of the skin resistance losses, the distribution of voltage along the length of the dee electrode, and a lumped-impedance equivalent circuit.

The effect of capacitive coupling between dees is analyzed for its influence on servotuning of the dees. A tuning function is presented which should make stable servotuning possible for any amount of dee-to-dee coupling.

A coupling network is considered that will permit coupling the power amplifiers to the dee stems with a short transmission line. The performance of this network is analyzed to find the optimum set of component values for a particular line length. Then, by means of an optimized coupling network, the available dee voltage is estimated for a particular dee-stem coupling point.

INTRODUCTION

The proposed modification of the Lewis Research Center cyclotron copies the design of the Princeton Azimuthally-Varying-Field Cyclotron. The analysis given in this report deals mainly with the resonant cavity of the Princeton machine which is nearly identical to that planned for the Lewis machine; in this sense it is an after-the-fact engineering calculation which has served an educational purpose. But the analysis has also provided new information which will be incorporated in the design of the new Lewis cyclotron.

The results of this work are divided into four parts. First, the resonant circuit of a single dee is considered. Then, dee-to-dee coupling effects are examined and a tuning

method is suggested which should improve servotuning of the dee panels. In the third section, a redesign of the amplifier-to-dee drive line is examined; and in the last section, amplifier-to-dee system performance is predicted for one particular combination of dee-stem tap point and coupling network.

The calculational methods used in these analyses are described in the following section.

METHOD OF ANALYSIS

The equivalent circuits representing the cyclotron dee system and drive lines can be regarded as several four-terminal networks in series. Each four-terminal network contains either lumped impedances or a segment of uniform transmission line. A computer code was devised to obtain the steady-state solution of this general problem by evaluating the impedances at the frequencies of interest and by reducing the circuit to a single four-terminal network with three independent impedances.

Impedances of a Four-Terminal Network

Consider the four-terminal network of figure 1 to contain only linear complex impedances and the complex currents in the two a-terminals to be equal (which must then also be true of the two b-terminals). Thus, there are only two currents that need be consid-

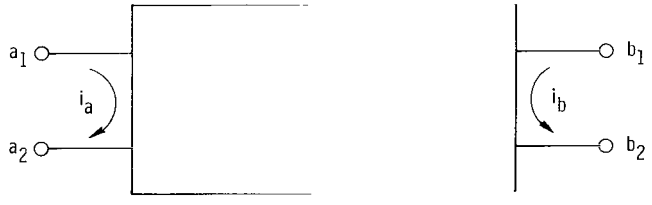

Figure 1. - Four-terminal network.

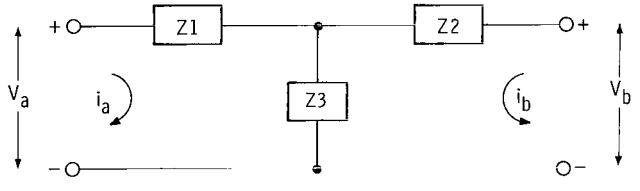

Figure 2. - Three-element circuit equivalent to four-terminal network of figure 1.

ered, i_a and i_b. It is shown in reference 1 that there is an equivalent three-element circuit for any such four-terminal network.

The important equations for the three-element circuit in figure 2 are

$$\left.\begin{aligned} V_a &= (Z1)(i_a) + (Z3)(i_a + i_b) \\ V_b &= (Z2)(i_b) + (Z3)(i_a + i_b) \end{aligned}\right\} \quad (1)$$

If three terminal impedances are defined as

$$ZAA \equiv \text{Input impedance} = Z1 + Z3$$

$$ZBB \equiv \text{Output impedance} = Z2 + Z3$$

$$ZAB \equiv \text{Mutual impedance} = Z3$$

then equations (1) become

$$\left.\begin{aligned} V_a &= (ZAA)(i_a) + (ZAB)(i_b) \\ V_b &= (ZBB)(i_b) + (ZAB)(i_a) \end{aligned}\right\} \quad (2)$$

Reduction of Two Networks in Series

Two four-terminal networks connected in series can be reduced to a single four-terminal network. The combined circuits in figure 3 can be reduced to the single net-

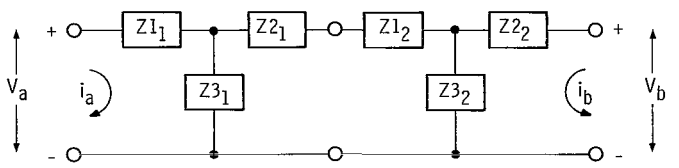

Figure 3. - Two networks connected in series.

work of figure 2 as follows:

Let

$$\left.\begin{aligned} ZAA_1 &= Z1_1 + Z3_1 \\ ZAA_2 &= Z1_2 + Z3_2 \\ ZAB_1 &= Z3_1 \\ ZAB_2 &= Z3_2 \\ ZBB_1 &= Z2_1 + Z3_1 \\ ZBB_2 &= Z2_2 + Z3_2 \end{aligned}\right\} \quad (3)$$

and

$$\left.\begin{aligned} ZN_1 &= ZAA_2 + ZBB_1 - ZAB_1 \\ ZN_2 &= ZBB_1 + ZAA_2 - ZAB_2 \\ YL &= \frac{1}{ZL} = \frac{1}{ZN_1} + \frac{1}{ZAB_1} \\ YR &= \frac{1}{ZR} = \frac{1}{ZN_2} + \frac{1}{ZAB_2} \end{aligned}\right\} \quad (4)$$

Then

$$\left.\begin{aligned} ZAA &= ZAA_1 - ZAB_1 + ZL \\ ZBB &= ZBB_2 - ZAB_2 + ZR \\ ZAB &= ZL \times \frac{ZAB_2}{ZN_1} \end{aligned}\right\} \quad (5)$$

where the unsubscripted impedances in equations (5) are the terminal impedances of the combined network that can be used in equations (2).

These operations can be repeated any number of times to reduce a series of four-terminal networks to a single network having only three impedances.

Equivalent Circuit for a Transmission Line

A length of uniform transmission line is also a four-terminal network and so it too can be represented by a three-element equivalent circuit. It is shown in reference 1 that if

f frequency, Hz

Z0 characteristic impedance, ohms

V phase velocity, m/sec

l length, m

α voltage attenuation (loss) coefficient, m^{-1}

then the three terminal impedances of the equivalent circuit are

$$ZAA = ZBB = Z0 \times \coth(ARG)$$

$$ZAB = Z0 \times \operatorname{csch}(ARG)$$

where

$$ARG \equiv \left(\alpha + j\frac{2\pi f}{V}\right) l$$

and j is a complex operator, coth is a hyperbolic tangent operator, and csch is a hyperbolic cosecant operator.

Description of Computer Code

A computer code was arranged to handle up to 99 three-element circuits in series. Naming of the individual lumped elements is indicated in figure 4. Any of the impedances in any section were allowed to take on values. Two special situations were recognized by the computer program: if any C = 0, it was assumed that the capacitor was to be replaced by a conductor; if L3, R3, and C3 all appeared as zero in a particular section, Z3 was taken to be infinite.

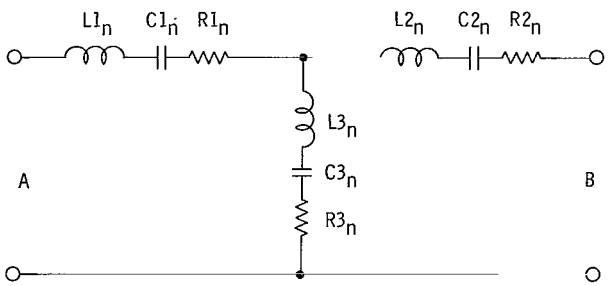

Figure 4. - Impedance elements in single network with nomenclature used in computer code.

The computer code recognized sections of transmission line by $l \neq 0$. In this case, the values of L, R, and C for that section were ignored and, instead, the values of characteristic impedance, velocity, and loss were used to evaluate the section impedances.

The program was arranged to sweep either the frequency or one of the section parameters through a number of values spaced by a constant fraction of the input value. If a parameter other than frequency was to be swept, this was signaled by making the input value of that parameter negative. Also included in the code was the provision to name a tap point between any two sections as the output terminal. This provision made voltage ratio calculations more convenient.

DEE-CIRCUIT ANALYSIS

The assembly consisting of a dee, a dee stem, and the surrounding cavity liners can be thought of as a transmission line, open circuited at the dee end and short circuited at the other (root) end. The impedance of the line varies along its length, particularly in the region of the tuning panels. The mechanical dimensions of this system were obtained from drawings and from a model of the panel system. Electrical parameters (impedance and loss coefficient) were then determined from these dimensions and used as input to the network impedance calculation. From the calculated terminal impedances for the entire dee-circuit network could then be obtained the resonant frequency, voltage distribution, and a lumped-impedance equivalent circuit (with skin losses).

Physical Dimensions

The width of the dees and the size of the gap between dee and liner varies along the dee length. For the present purpose, these variations were accounted for by dividing the

TABLE I. - MECHANICAL DIMENSIONS OF DEE-LINER SECTIONS

Section	Section center, cm from root	Section length, cm	Section width, b, cm	Actuator extension, cm							
				0	2.16	4.32	9.14	15.62	22.40	31.29	43.82
				Vacuum gap dimension d for each of eight panel positions, cm							
				1	2	3	4	5	6	7	8
1	279.4	12.7	16.8	3.39	3.39	3.39	3.39	3.39	3.39	3.39	3.39
2	266.7	↓	37.3	↓	↓	↓	↓	↓	↓	↓	↓
3	254.0		50.8								
4	241.3		61.0								
5	228.6		68.6								
6	215.9		72.4								
7	203.2		69.1								
8	190.5		63.0								
9	177.8		57.4								
10	165.1	↓	51.6								
11	114.3	89.2	47.5	↓	↓	↓	↓	↓	↓	↓	↓
12	67.3	4.6	47.2	31.75	31.75	31.75	31.75	31.75	31.75	31.75	31.75
13	63.0	4.1	↓	1.78	2.24	2.72	13.34	25.78	28.27	30.86	↓
14	58.4	5.1		↓	2.67	3.23	3.53	14.61	22.07	27.31	
15	53.3	↓			3.23	4.34	5.31	5.92	15.11	23.29	
16	48.3				3.84	5.44	7.49	8.00	9.45	19.18	
17	43.2				4.39	6.58	9.78	11.05	11.35	15.21	
18	38.1				4.95	7.67	11.96	14.15	14.76	16.18	
19	33.0			↓	5.51	8.81	14.20	17.30	18.16	19.33	
20	27.9			1.80	5.51	9.42	16.18	20.40	21.62	22.53	
21	22.9			1.98	5.08	8.20	14.48	22.17	25.10	25.68	
22	17.8			2.16	4.60	7.04	11.91	18.52	26.49	28.88	
23	12.7		↓	2.31	4.09	5.84	9.58	14.05	20.12	30.66	
24	7.6		53.3	2.54	3.58	4.65	7.01	9.63	13.26	22.86	
25	2.5	↓	66.8	2.74	3.10	3.43	4.17	5.21	6.30	9.53	↓

entire length into 25 segments, each of which was then treated as though its dimensions were uniform along the length axis.

Table I lists all of the mechanical dimensions used in this analysis. The dee and dee-stem dimensions given in table I were taken from the 1/4 scale drawing of the north dee assembly. The schedule of gap dimensions over the panel region (sections 12 to 25) were obtained from a 1/2 scale model of the panel linkage. Eight different positions were used, ranging from fully closed (position 1 with actuator extension of 0 in.) to fully open (position 8 with actuator extension of 43.82 cm).

Electrical Parameters

In figure 5 a typical dee-liner cross section is compared with a strip line. A strip line consists of a conducting ribbon between two infinite conducting planes. In refer-

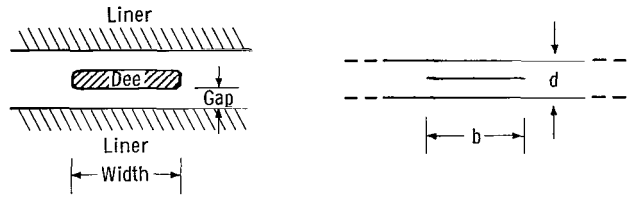

(a) Dee-liner cross section. (b) Strip-line cross section.

Figure 5. - Comparison of cross sections of cyclotron dee-liner assembly with strip line. (Dimensions shown for strip line are those used in eq. (6) for strip-line impedance.)

ence 2, the impedance of a strip line with vacuum dielectric is given as

$$Z_0 = \frac{30\pi K(k)}{K'(k)} \text{ ohms} \tag{6}$$

where K(k) is the complete elliptic integral of module

$$k = \frac{1}{\cosh\left(\frac{\pi}{2} \times \frac{b}{d}\right)}$$

and where $K'(k) = K\left(\sqrt{1 - k^2}\right)$.

For values of d/b less than 0.3, equation (6) is best evaluated by the approximation

$$Z_0 = \frac{15\pi^2}{\ln 2 + \left(\frac{\pi}{2}\right)\left(\frac{b}{d}\right)} \tag{6a}$$

Table II lists some calculated values of Z_0 for selected values of d/b.

The actual dee-liner cross section differs from a true strip line in two ways. First, the liners are not infinite in extent. But they are wide enough that liner edge effects should be unimportant, even in the panel region where the gap dimension is quite large. The second matter is the thickness of the dees (6.35 cm). In order to use equation (6),

TABLE II. - CALCULATED STRIP-LINE IMPEDANCES (FOR GEOMETRY SHOWN IN FIG. 5)

Ratio of gap dimension to width, d/b	Characteristic impedance, Z0, ohms
0.010	0.938
.022	2.054
.047	4.340
.068	6.222
.100	9.026
.15	13.26
.22	18.90
.33	27.15
.47	36.69
.68	49.30
.82	56.75
1.00	65.40
1.2	73.97
1.5	85.16
1.8	94.78
2.2	105.8
2.7	117.3
3.3	128.8
3.9	138.5

TABLE III. - DEE-LINER SECTION IMPEDANCES

Section	Section length, m	Section impedances for each of eight panel positions, ohms							
		1	2	3	4	5	6	7	8
1	0.127	33.0	33.0	33.0	33.0	33.0	33.0	33.0	33.0
2		15.9	15.9	15.9	15.9	15.9	15.9	15.9	15.9
3		11.9	11.9	11.9	11.9	11.9	11.9	11.9	11.9
4		10.0	10.0	10.0	10.0	10.0	10.0	10.0	10.0
5		8.9	8.9	8.9	8.9	8.9	8.9	8.9	8.9
6		8.45	8.45	8.45	8.45	8.45	8.45	8.45	8.45
7		8.85	8.85	8.85	8.85	8.85	8.85	8.85	8.85
8		9.65	9.65	0.65	0.65	0.65	9.65	9.65	9.65
9		10.7	10.7	10.7	10.7	10.7	10.7	10.7	10.7
10		11.8	11.8	11.8	11.8	11.8	11.8	11.8	11.8
11	.891	12.7	12.7	12.7	12.7	12.7	12.7	12.7	12.7
12	.0457	80.0	80.0	80.0	80.0	80.0	80.0	80.0	80.0
13	.0406	6.84	8.55	10.4	43.0	70.0	74.5	79.0	80.0
14	.0508		10.2	12.1	13.1	46.0	63.0	72.0	
15			12.1	16.1	19.3	21.2	47.3	66.0	
16			14.3	19.7	26.2	27.8	32.3	57.2	
17			16.2	23.3	33.2	36.7	37.1	48.0	
18			18.1	26.9	39.2	45.0	46.4	50.0	
19			20.0	30.3	45.2	52.7	55.4	57.3	
20		6.95	20.0	32.4	50.0	59.6	62.3	64.0	
21		7.60	18.4	28.3	46.0	63.3	68.5	70.0	
22		8.35	16.8	24.8	39.0	55.6	71.6	76.0	
23		8.80	15.2	21.0	32.5	44.5	58.8	78.2	
24		8.60	11.9	15.3	22.3	29.4	38.0	59.0	74.2
25		7.42	8.4	9.3	11.2	13.6	16.3	24.0	64.0

the plane spacing d should be taken to be twice the dee-to-liner gap dimension. This still leaves edge fields incompletely accounted for, but they should be relatively unimportant for the dee-liner geometry because the dee width is much greater than the dee thickness. Table III lists all of the section impedances corresponding to entries in table I.

Dee losses were obtained from the digital computer calculation by including the loss coefficient of each segment. From reference 1 (p. 144), the loss coefficient for transverse electromagnetic waves between parallel conducting planes is given by

$$\alpha_{tem} = \frac{1}{s}\sqrt{\frac{\epsilon_0}{\mu_0}}\sqrt{\frac{\mu\omega}{2\sigma}} \qquad (7)$$

where

s plane spacing

ϵ_0 dielectric constant of vacuum

μ_0 permeability of vacuum

μ permeability of planes

ω $2\pi \times$ frequency

σ conductivity of planes

Equation (7) does not precisely apply to the true dee-liner geometry, again because edge effects are ignored. But since the dee width is much greater than the dee thickness, equation (7) should be adequate to estimate the losses that will occur. If it is assumed that $\mu = \mu_0$, equation (7) becomes

$$\alpha = \frac{1}{s}\sqrt{\frac{\epsilon_0 \omega}{2\sigma}} \tag{8}$$

Table IV lists the loss coefficients for each dee section at each of eight frequencies cor-

TABLE IV. - DEE-LINER SECTION LOSS COEFFICIENTS

Section	Frequencies for resonance, MHz							
	25.71	22.93	21.15	18.82	17.17	16.17	15.17	13.81
	Section loss coefficients for each of eight panel positions, m^{-1}							
	1	2	3	4	5	6	7	8
1 to 11	1.036×10^{-4}	0.978×10^{-4}	0.940×10^{-4}	0.886×10^{-4}	0.846×10^{-4}	0.821×10^{-4}	0.797×10^{-4}	0.759×10^{-4}
12	.111	.105	.100	.095	.090	.088	.085	.081
13	1.975	1.484	1.173	.225	.111	.098	.087	↓
14	↓	1.244	.988	.851	.196	.126	.099	↓
15	↓	1.028	.734	.566	.485	.184	.116	↓
16	↓	.865	.586	.401	.359	.295	.141	↓
17	↓	.755	.484	.307	.260	.245	.178	↓
18	↓	.670	.415	.251	.203	.189	.167	↓
19	↓	.602	.362	.212	.166	.153	.140	↓
20	1.947	.602	.338	.159	.141	.129	.120	↓
21	1.773	.653	.389	.208	.129	.111	.105	↓
22	1.626	.722	.451	.252	.155	.105	.094	↓
23	1.520	.811	.545	.314	.204	.138	.088	↓
24	1.383	.926	.686	.429	.298	.210	.118	↓
25	1.280	1.070	.929	.722	.551	.442	.284	↓

responding to the eight panel positions. These values were obtained from equation (8), using $\epsilon_0 = 8.85\times10^{-12}$ F×m^{-1} and $\sigma = 5.8\times10^{7}$ Ω^{-1}m^{-1}.

Results of Dee-Circuit Analysis

The resonant frequency of each of the eight panel positions was obtained first by search for the lowest (but not zero) frequency at which the dee-circuit terminal impedances were purely resistive. For this calculation, the skin resistance need not be accurately known because it is so small compared to the capacitive and inductive reactances. In table V are listed the resonant frequencies for the eight panel positions that

TABLE V. - ACTUATOR EXTENSIONS AND RESONANT FREQUENCIES FOR EACH OF EIGHT PANEL POSITIONS

Panel position	Actuator extension, cm	Frequency, MHz
1	0	25.71
2	2.16	22.93
3	4.32	21.15
4	9.14	18.82
5	15.62	17.17
6	22.40	16.17
7	31.29	15.17
8	43.82	13.81

result from the lengths and section impedances of table III. In figure 6 the variation of resonant frequency with actuator position is plotted graphically.

The computer code could also be used to obtain the voltage distribution along the dee and dee stem. This was done by mathematically connecting a tap point between two line segments and the output terminals of the network (shown schematically in fig. 7). The results of these calculations are listed in table VI and are shown graphically in figures 8 and 9.

The voltage distributions over the dees in figure 8 are used to relate the average dee voltage seen by accelerated particles to the dee-tip voltage. The calculation of this ratio is discussed in the appendix. The voltage distributions on the dee stem in figure 9 are used to determine the tap point connection to the radiofrequency amplifier. This connection point is located so as to provide the desired load impedance for the power amplifier.

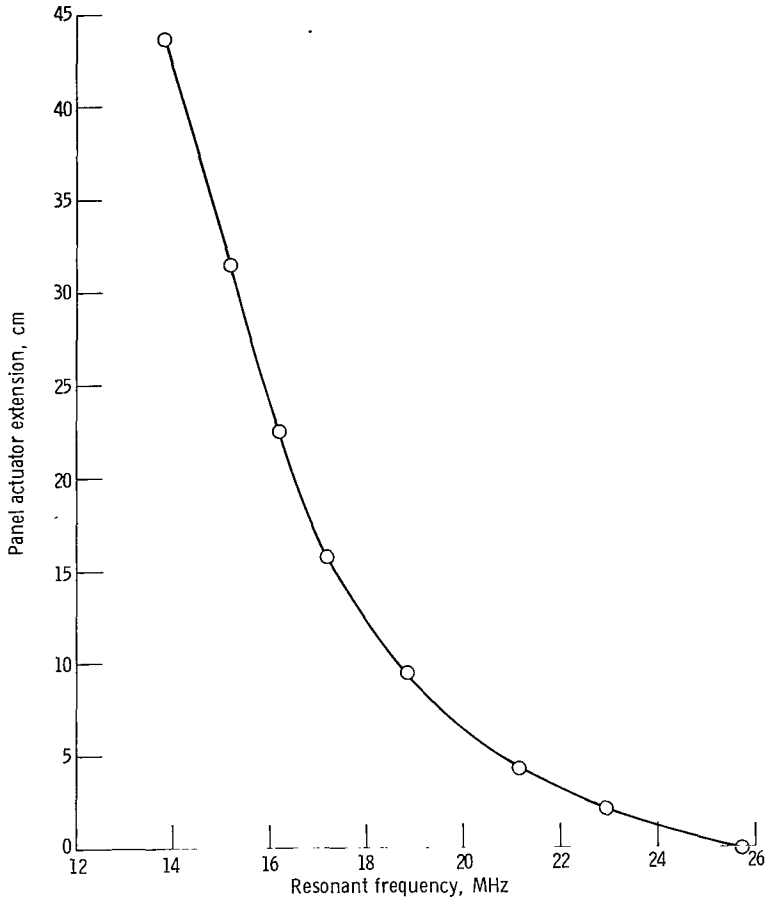

Figure 6. - Dee circuit resonant frequency against panel actuator extension.

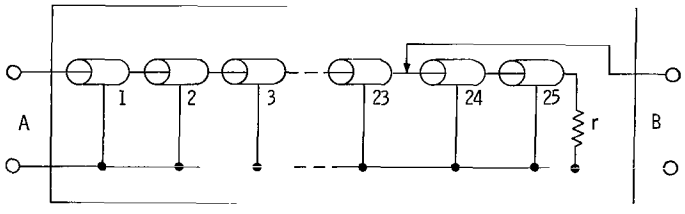

Figure 7. - Schematic arrangement of transmission line sections used in dee-circuit calculations. Location of tap point could be varied.

TABLE VI. - DEE AND DEE-STEM VOLTAGES (NORMALIZED TO UNITY TIP VOLTS) AT A NUMBER OF TAP POINTS

Tap point, m from root	Tap point voltage for each of eight tuning panel positions							
	1	2	3	4	5	6	7	8
2.731	0.9977	0.9981	0.9984	0.9987	------	------	0.9992	------
2.604	.9931	.9945	.9953	.9963	------	------	.9976	------
2.477	.9856	.9885	.9902	.9922	------	------	.9950	------
2.350	.9750	.9801	.9830	.9866	------	------	.9913	------
2.223	.9613	.9692	.9737	.9792	------	------	.9864	------
2.096	.9440	.9553	.9619	.9699	------	------	.9803	------
1.969	.9212	.9371	.9463	.9574	------	------	.9722	------
1.842	.8919	.9137	.9262	.9415	------	------	.9618	------
1.715	.8550	.8840	.9009	.9213	------	------	.9486	------
1.588	.8102	.8479	.8699	.8966	------	------	.9323	------
.508	.1760	.3080	.3893	.4683	0.4889	0.4963	.5260	0.5866
.406	.1446	.2497	.3176	.3883	.4158	.4256	.4319	.4666
.305	.1129	.1762	.2215	.2738	.3045	.3221	.3354	.3462
.254	.0965	.1375	.1669	.2058	.2364	.2586	.2777	.2858
.203	.0786	.1018	.1191	.1432	.1639	.1887	.2144	.2254

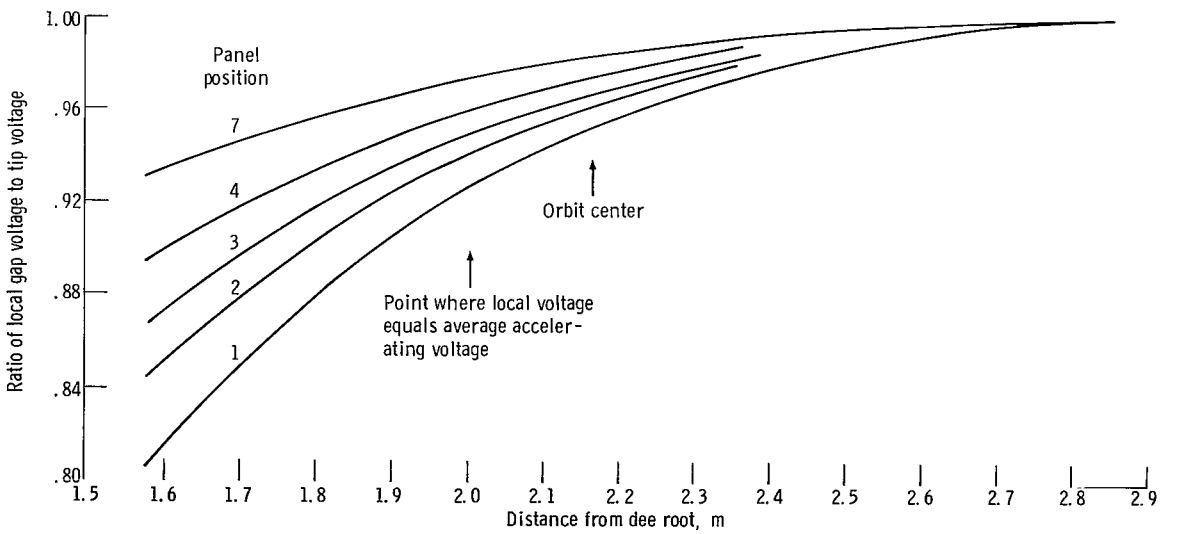

Figure 8. - Variation of dee voltage in region of accelerating gap.

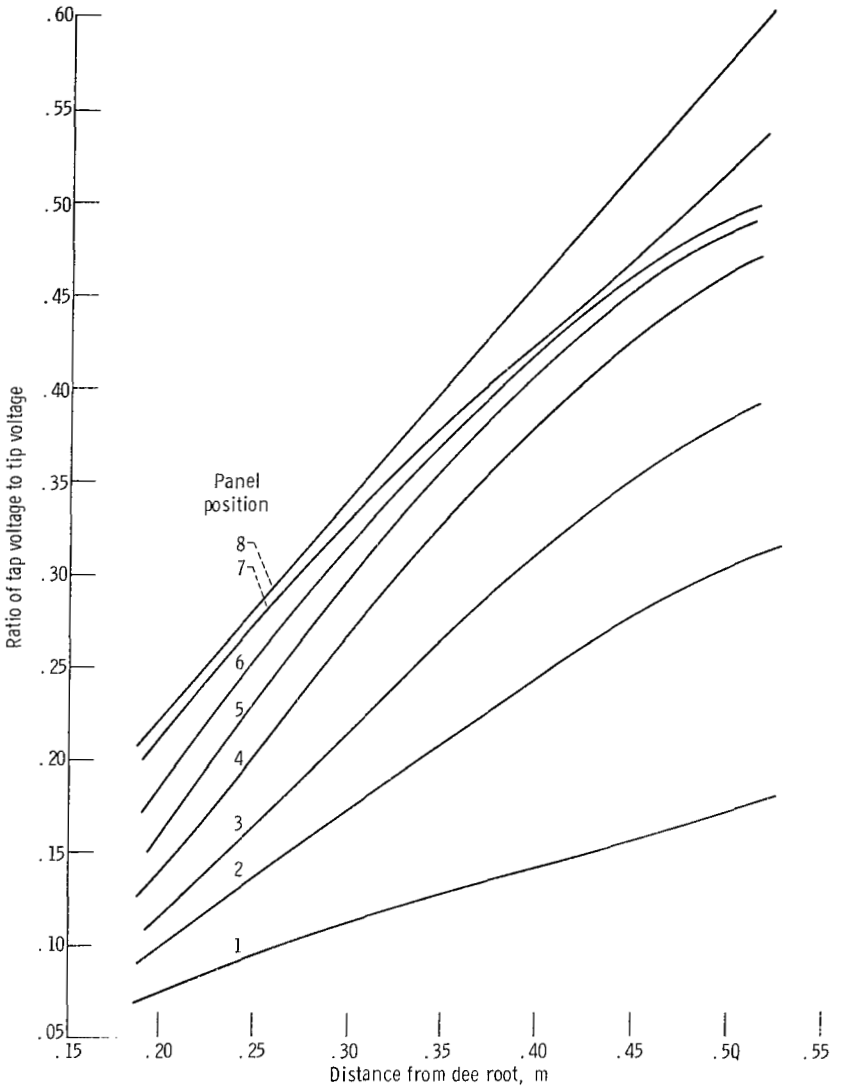

Figure 9. - Variation of voltage along dee stem.

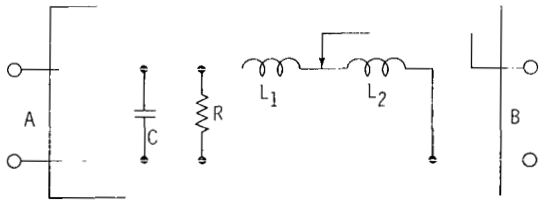

Figure 10. - Simplified equivalent circuit used to represent dee-liner system.

Further analyses involving the dee circuit can be simplified by replacing the transmission line representation of figure 7 with the equivalent circuit of figure 10. In this circuit, the distributed capacity of the dee and dee stem are lumped at the tip (terminals A). The inductance of the dee stem is divided between L_1 and L_2 by the tap point. The resistor R is the lumped equivalent of the skin losses and C is a convenient representation of the system capacity. The values of these parameters at a particular panel position (and hence frequency) are obtained from the computed terminal impedances of the circuit in figure 7 since the circuit of figure 10 must have the same terminal impedances if it is to be equivalent.

By means of a small test resistance (r in fig. 7), the current at the dee root per unit tip voltage V_a could be obtained. This current must be equal to the total displacement current between dee and liner (at the fundamental resonant frequency). In the simplified circuit of figure 10, all of this displacement current flows in C. From the equation

$$X_c = \frac{V}{I} = \frac{1}{2\pi fC} \tag{9}$$

for capacitive reactance X_c, C can be determined by using tip volts for V and root amperes for I.

From C, the total inductance $L_1 + L_2$ can be calculated by

$$2\pi f(L_1 + L_2) = \frac{1}{2\pi fC} \tag{10}$$

TABLE VII. - VALUES OF LUMPED IMPEDANCES

THAT MAKE CIRCUIT OF FIGURE 10

EQUIVALENT TO FIGURE 7

Frequency, MHz	Capacitance, C, pF	Total inductance, $L_1 + L_2$, μH	Resistance, R, kΩ
25.71	536.5	0.0714	36.5
22.93	554.0	.0869	40.7
21.15	566.0	.1000	43.8
18.82	576.0	.1241	49.1
17.17	581.0	.1480	53.5
16.17	584.0	.1659	56.4
15.17	587.5	.1874	59.2
13.81	592.0	.2243	64.1

because the two reactances must have equal magnitude at resonance. And the resistor R must equal the terminal impedance ZAA at resonance. The values calculated at the eight frequencies are given in table VII.

DEE-TO-DEE COUPLING EFFECTS

In the Princeton AVF Cyclotron, two dees are used and each is driven by its own power amplifier. Preliminary data obtained from the Princeton machine indicates that dee-to-dee coupling is small but not negligible; as a result, changes in the dee-tuning and dee-voltage control systems were necessary. In this section, dee-to-dee coupling effects are examined so that a suitable control system function can be found.

Equivalent Circuit for Dual-Drive System

The four-terminal network equivalent circuit used to analyze dee-to-dee coupling effects is shown in figure 11. In this circuit, each dee is represented by a parallel reso-

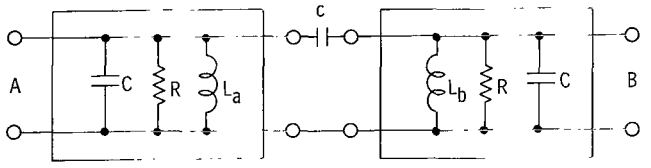

Figure 11. - Equivalent circuit used in analysis of dee-to-dee coupling effects.

nant circuit similar to that of figure 10, where the total dee-stem inductance (L_A or L_B) in figure 11 is equal to $L_1 + L_2$ in figure 10. The small capacitor c is sized to give the desired dee-to-dee coupling.

The power amplifiers that drive the dees of the Princeton cyclotron can be thought of as radiofrequency current sources; the high plate resistance of the 4CW100,000D tetrode vacuum tubes gives these amplifiers a high internal impedance. The equations for dee voltage

$$\left.\begin{aligned} V_a &= (ZAA)(i_a) + (ZAB)(i_b) \\ V_b &= (ZBB)(i_b) + (ZAB)(i_a) \end{aligned}\right\} \qquad (2)$$

can then be evaluated, allowing that i_a is the radiofrequency current from the A-side amplifier and i_b the current from the B-side amplifier. (The amplifier currents are not really injected at the dee tips, of course; but the impedance ratio between the dee tip and the amplifier drive point varies relatively slowly with frequency and this transformation can be considered as part of the amplifier.)

The power amplifiers are driven equally either in phase (push-push mode) or 180^o out of phase (push-pull mode). In the push-push mode, $i_a = i_b$ and the dee voltages are given by

$$\left.\begin{aligned} V_a &= (ZAA + ZAB)i_a \\ V_b &= (ZBB + ZAB)i_b \end{aligned}\right\} \quad \text{Push-push mode} \tag{11}$$

In the push-pull mode, $i_a = -i_b$ and the dee voltages are given by

$$\left.\begin{aligned} V_a &= (ZAA - ZAB)i_a \\ V_b &= (ZBB - ZAB)i_b \end{aligned}\right\} \quad \text{Push-pull mode} \tag{12}$$

The network impedances in equations (11) and (12) are easily obtained for the equivalent circuit of figure 11.

Tuning Plane Impedance Behavior

The aim of dee tuning is to make the dee voltages equal in magnitude and in phase with their respective driving amplifier currents. If the two dee circuits in figure 11 are assumed to be identical, then for any given set of values for R, C, and L there are two frequencies at which these tuning conditions are satisfied: one for each of the two modes of operation. The difference between these two frequencies is proportional to the amount of dee-to-dee coupling present. This frequency difference, known as mode separation, is commonly used as a measure of coupling strength.

Preliminary data from the Princeton cyclotron indicates that the dee-to-dee coupling is strong enough to separate the modes by several kilohertz. The results that follow were calculated by assuming the capacitive coupling (c in fig. 11) to be 0.2 picofarad, sufficient to cause a 6.5-kilohertz mode separation at 21 megahertz.

Figure 12 shows a contour plot of the quantity ZAA + ZAB (the left-dee voltage normalized to unit driving current in the push-push mode). In this figure the values of L_a and L_b in the equivalent circuit of figure 11 are considered as independent variables. The values of C and R are those given in table VII for a 21.15-megahertz resonant fre-

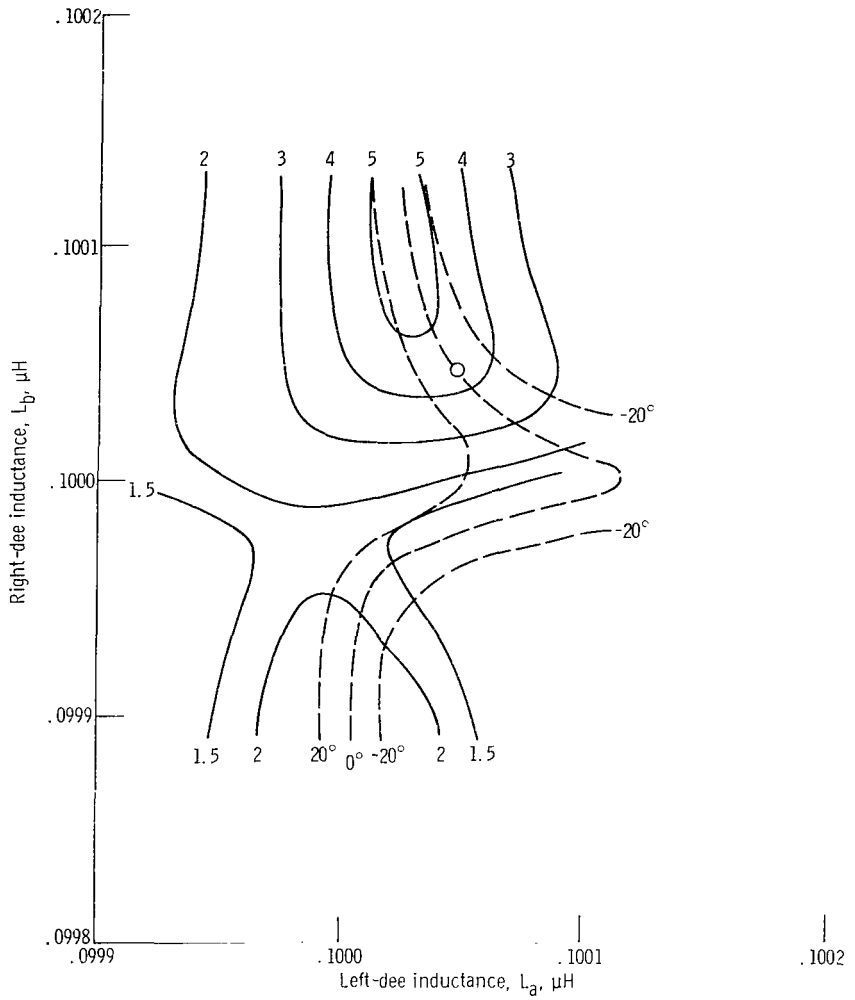

Figure 12. - Tuning plane plot of left-dee impedance parameter ZAA + ZAB for push-push mode. Dee-to-dee coupling, 0.2 picofarad; frequency, 21.15 megahertz. Solid lines are contours of constant modulus (10^4 ohms); dashed lines are contours of constant phase angle.

quency. Three-dimensional surfaces would be needed to give a complete description of the modulus and phase angle of the dee impedance in the field of the independent variables L_a and L_b. In figure 12, these surfaces are suggested by showing the surface height contours. Near the center of the plot a small circle marks the location of the tuning point at which the left- and right-dee voltages are equal in phase and magnitude.

If the dee-to-dee coupling were zero, a contour plot of the left-dee impedance, such as that in figure 12, would be just a series of vertical lines; the left-dee impedance would not depend on the right-dee inductance. The great difference between this limiting case and the results of figure 12 emphasize how sensitive the dee circuits are to a little dee-to-dee coupling.

Tuning Function Behavior

In the limit of zero dee-to-dee coupling, tuning of the dees is done by adjusting the dee inductance (panel position) to obtain zero phase difference between the dee voltage and the driving current. But with dee-to-dee coupling present, this procedure may not work. In figure 12, the 0^{o} phase contour is a very curvy line, showing that the phase of the left-dee voltage is strongly dependent on the tuning of the right dee. Some tuning function other than just phase is required for this situation. There are three requirements of a satisfactory tuning function:

(1) It must lead to the correct in-tune point; the dee voltages should be equal in magnitude and in phase with their respective driving amplifier currents.

(2) It should be such that the left-dee tuning function does not vary with right-dee tuning and the reverse.

(3) It should be easy to generate as an analog voltage signal.

A tuning function which, it is believed, satisfactorily meets these requirements has been devised. It is

$$\left.\begin{aligned} \mathrm{TUNE}_L &= \theta_L + K\left(\ln|V_L| - \ln|V_R|\right) \\ \mathrm{TUNE}_R &= \theta_R + K\left(\ln|V_R| - \ln|V_L|\right) \end{aligned}\right\} \qquad (13)$$

where θ is the phase angle (in radians) of the dee voltage relative to the driving current, $|V|$ is the amplitude of the dee voltage, K is a constant, and the subscripts L and R refer to the left- and right-dee values.

Equations (13) were evaluated for the same equivalent circuit values used to produce figure 12. Contour lines of the left and right tuning functions are shown in figure 13. The value of $K = 1.0$ used in equations (13) was determined by trial to make the $\mathrm{TUNE}_L = 0$ and $\mathrm{TUNE}_R = 0$ contour lines orthogonal at the in-tune point marked by the small circle. Figure 13 shows that requirements a and b are satisfied, at least in the neighborhood of the in-tune point. Furthermore, simple logarithmic amplifiers are available for generating the logarithms indicated in equations (13).

Calculations have been made which show that the value of K that makes the left and right tuning functions orthogonal is porportional to the strength of dee-to-dee coupling. The sign of K depends on whether the mode is push-push or push-pull, being positive for whichever mode has the higher resonant frequency.

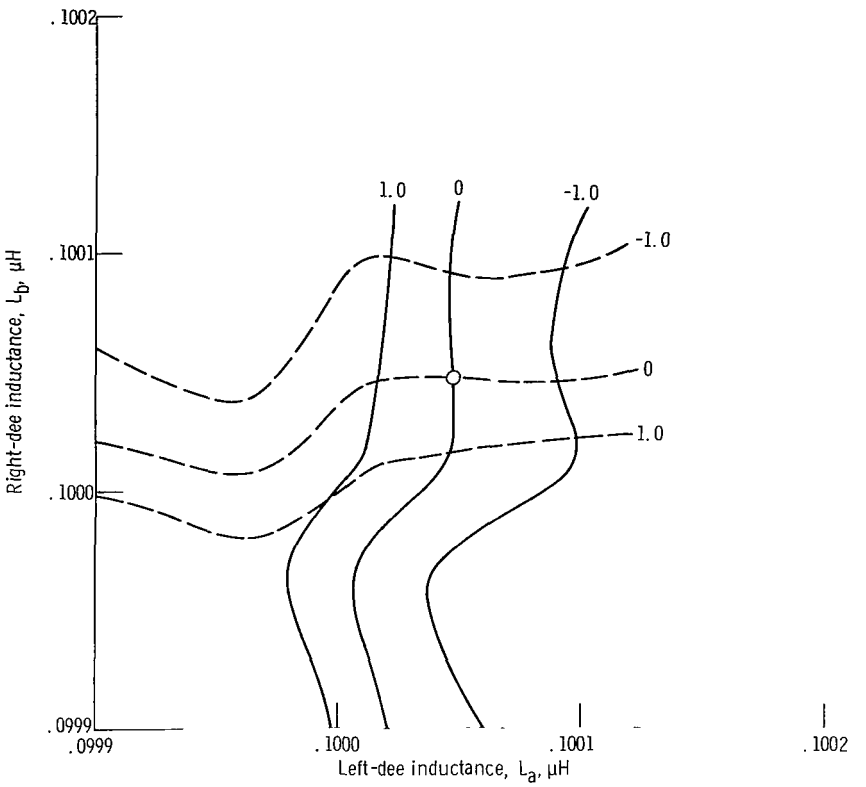

Figure 13. - Tuning plane plot of tuning function for push-push mode. Dee-to-dee coupling, 0.2 picofarad; frequency, 21.15 megahertz. Solid lines are contours of constant left-dee tuning function; dashed lines are contours of contstant right-dee tuning function.

LENGTH EFFECTS IN AMPLIFIER-TO-DEE TRANSMISSION LINE

The power amplifiers that drive the dees of the Princeton cyclotron are located at some distance above the panel tuning cavity and outside of the radiation shield. Between the amplifiers and the dees are two tuned, half-wave transmission lines, one for each dee. This arrangement was chosen so that the power amplifiers would be accessible at all times for maintenance. For the Lewis cyclotron, it is not feasible to arrange a tuned line long enough to put the power amplifiers outside of the shield vault. Instead, it is better to eliminate the half-wave line section of the Princeton design and to keep the amplifier-to-dee connection as short as possible.

If the power amplifiers are placed directly on top of the vacuum box containing the tuning panels, the shortest coupling possible between the amplifier and the dee stem would be a transmission line approximately 0.9 meter long plus the coupling tap bar with a length of approximately 0.4 meter. These lengths make the coupling system a very significant circuit element in the frequency range over which the cyclotron is to operate. Large reactive currents will be encountered because of the impedance transforming ef-

fects of a length of transmission line. Other important line-length effects are the voltage ratio and the phase lag between source and load ends.

The most critical part of the amplifier-to-dee coupling is the tap bar. This bar is not directly cooled. Any heat generated in it due to skin resistance must be conducted to the ends, where the heat can be carried away by the water cooling provided there. The way to minimize heating in this bar is to adjust the circuit parameters so that the impedance at its center is purely resistive. Then the current will be a minimum for a given power transfer. Such a circuit is shown in figure 14.

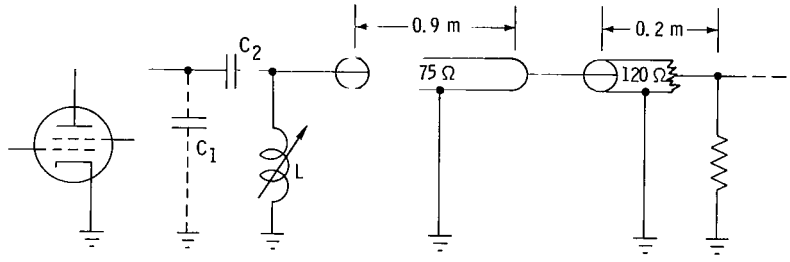

Figure 14. - Amplifier-to-dee-tap coupling network used to minimize tap-bar heating.

The coupling bar can be thought of as a section of transmission line, the impedance of which varies with the position of the nearby tuning panels. In the Lewis cyclotron, this impedance approximates 120 ohms, being highest at the lowest resonant frequency. The coupling line between the tap bar and the driver amplifier has an impedance of 75 ohms. In figure 14, the 0.2-meter length is the distance from one end of the tap bar to its center, where the impedance is to be purely resistive. The other elements in figure 14 are the power-amplifier-tube anode capacitance C_1, the direct-current blocking capacitance C_2, and a tuning inductance L, used to balance out all of the capacitive reactance from C_1 and the transmission line.

Table VIII gives the results of impedance calculations of the coupling network of figure 14 with $C_1 = 70$ picofarads and $C_2 = 1000$ picofarads. The inductance values given make the amplifier-tube anode impedance purely resistive. If the load in figure 14 is considered to be part of the coupling network, then in equations (2), $i_b = 0$ and the voltage ratio between the tap bar and the amplifier-tube anode becomes

$$\frac{V_{tap}}{V_{anode}} = \frac{ZAB}{ZAA} \tag{14}$$

Similarly, the voltage across the inductor normalized to unit input voltage (1.070) can be

TABLE VIII. - COUPLING NETWORK PARAMETERS FOR CIRCUIT OF FIGURE 14 WITH C_1 = 70 pF AND C_2 = 1000 pF

Frequency, MHz	Inductance, μH	Voltage ratio, V_{tap}/V_{anode}		Inductor current at 10-kV input terminal voltage, I_L/V_{anode}, A per 10 kV
		Modulus	Phase, deg	
25.71	0.330	1.259	-2.6	202
22.93	.420	1.217	-2.2	177
21.15	.496	1.193	-1.9	162
18.82	.630	1.166	-1.6	144
17.17	.761	1.149	-1.3	130
16.17	.860	1.139	-1.2	122
15.17	.980	1.131	-1.0	115
13.81	1.183	1.120	-.8	104

obtained. The last column in the table gives the inductor current at an input terminal voltage of 10 kilovolts.

The performance of the cyclotron radiofrequency (rf) system is described by the maximum attainable dee voltage as a function of frequency. This will depend on maximum power available from the driver amplifier, the particular tap point location on the dee stem, and the resistive losses actually encountered. In the remainder of this section a predicted performance is presented, a performance based on assumed values for each of these factors. This analysis further illustrates the nature of the cyclotron rf system.

For this calculation, it was assumed that each of the rf amplifiers could deliver 100 kilowatts into a 950-ohm resistive load. These conditions are based on the manufacturer's data sheets for the 4CW100,000D tube, assuming a 16-kilovolt direct-current anode voltage and class AB operation. The amplifier load can always be made purely resistive by proper dee tuning but, for a fixed dee-stem tap point, the 950-ohm load resistance can be had at only one frequency. It is therefore necessary to consider off-design operation of the amplifier tubes.

At a power of 100 kilowatts into 950 ohms, the rf anode voltage is 9.75 kilovolts and the rf current (fundamental component) is 10.25 amperes. (Radiofrequency voltages and currents are all given as rms values.) These values represent tube limits: higher voltages will cause excessive screen grid current, and higher load currents are possible only by drawing control grid current. Only at 950 ohms are these two limits reached together.

The total effect of these amplifier output limits can best be seen in the system performance results plotted in figure 15. The upper curve in figure 15 is the result of the calculation under discussion. At the peak point of this curve, the maximum 100 kilowatts

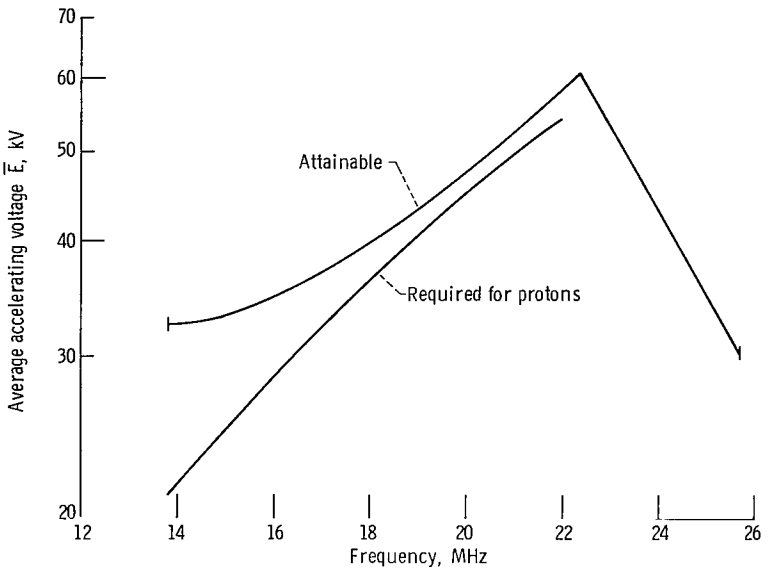

Figure 15. - Comparison of dee voltage required to accelerate protons and voltage attainable with dee-stem tap point 0.292 meter from dee root.

of power is delivered to the dee circuit. To the left of this point, at lower frequencies, the load resistance seen by the amplifier is greater than 950 ohms, and so the amplifier is operating at its voltage limit even though at reduced anode current. To the right of the maximum voltage point, the load reflected back to the amplifier is less than 950 ohms and the amplifier is delivering the full rf current but at a reduced rf voltage.

The dee-stem tap point used to get the upper curve in figure 15 was picked to give a small margin between the attainable dee voltage and the required dee voltage at a frequency of 21.15 megahertz. (The required voltage curve of fig. 15 was taken from orbit code calculations.) This tap point turned out to be 0.292 meter from the dee root.

Once a tap point is picked, the factor relating the amplifier rms anode voltage to average accelerating voltage is found from

$$\frac{\bar{E}}{V_{anode}} = \left(\frac{V_{tap}}{V_{anode}}\right) \times \left(\frac{V_{tip}}{V_{tap}}\right) \times \left(\frac{\bar{E}}{V_{tip}}\right) \tag{15}$$

where the three ratios in parentheses on the right are obtained from table VIII, figure 9, and figure 17, respectively. (Refer to the appendix for a discussion of the relation between the average accelerating-gap voltage $\bar{E}$ and V_{tip}.)

The anode load resistance is related to the skin loss resistance R given in table VII by

$$R_{anode} = R \times \left(\frac{V_{tap}}{V_{anode}} \times \frac{V_{tip}}{V_{tap}} \right)^{-2} \tag{16}$$

If the calculated anode load is less than the nominal 950 ohms, the anode voltage is found from the product of anode load resistance and the anode rf current (10.25 A). If the load resistance is greater than 950 ohms, the anode voltage is the limiting value of 9.75 kilovolts.

At frequencies above the maximum point of figure 15, the amplifier efficiency is reduced because of the reduced anode rf voltage. For example, at 25.71 megahertz, the anode rf voltage is only 2.8 kilovolts under the assumptions leading to figure 15. The power delivered to a dee at this frequency is only 29 kilowatts, but the total power input to the amplifier is the full 152 kilowatts, the same as it is when operating at 950 ohms load and 100 kilowatts output. The 123 kilowatts difference must be absorbed in the amplifier tube anode, but this is more than its 100 kilowatts rating. One way to avoid this problem is to reduce the direct-current anode voltage while maintaining the same anode current. The power input to the anode will be reduced without reducing the power delivered to the dee circuit.

SUMMARY OF RESULTS

A digital computer program has been devised to solve numerically for the terminal impedances of any four-terminal network. It has been applied to networks representing various parts of the radiofrequency system in the modified Lewis Research Center cyclotron.

Circuit element values used in these network representations have been derived from dimensions of the parts involved. The results of the terminal impedance calculations have to be used to obtain the following quantities:

1. The resonant frequency of the dees as a function of tuning panel position
2. The effects of dee-to-dee coupling on dee tuning
3. A dee voltage function which should permit stable automatic dee tuning
4. Optimum circuit parameters for a shortened coupling line between the radiofrequency amplifiers and the dee-stems
5. Predicted performance for a dee-stem tap point optimized for proton acceleration

Lewis Research Center,
National Aeronautics and Space Administration,
Cleveland, Ohio, August 25, 1969,
129-02.

APPENDIX - CALCULATION OF AVERAGE ACCELERATING VOLTAGE

Current operating practice is to adjust the cyclotron magnetic field and dee voltage so that particle orbits in the machine are the same no matter what kind of particles are being accelerated or what the extraction energy is. The correct field strength and dee voltage for a particular particle-energy combination are calculated by a digital computer program. In this calculation the voltage at the accelerating gap is assumed to be constant for all orbit radii. But in fact, the voltage along the gap is not constant.

In figure 8 (p. 13), the dee voltage in the region of the accelerating gap is plotted against distance from the dee root; five curves that correspond to five panel positions are shown. To a good approximation, the accelerating voltage over the dee varies as

$$V(\delta) = V_T(1 - \xi \delta^2) \tag{A1}$$

where

V_T tip voltage

δ distance from dee tip (measured along dee axis)

ξ function of frequency only

We need to know what the effective accelerating voltage of the dee is in view of this variation. In other words, for a given tip voltage, what is the average gap voltage seen by a single particle during a complete acceleration lifetime?

Since the particle orbits a point some distance from the dee tip, the gap voltage may be conveniently expressed in terms of orbit radius instead of the distance from the dee tip.

As shown in figure 16, where

δ_0 distance from orbit center to dee tip (measured along dee-stem axis)

β angle between accelerating gap edge and dee stem axis is

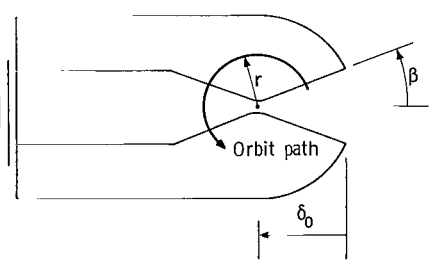

Figure 16. - Plan view of dee assembly showing dimensions used in calculating average accelerating voltage.

the voltage at orbit radius r on the tip side of the orbit center is

$$V^+ = V_T\left[1 - \xi\left(\delta_0 - r\cos\beta\right)^2\right] \tag{A2}$$

and on the root side of the orbit center it is

$$V^- = V_T\left[1 - \xi\left(\delta_0 + r\cos\beta\right)^2\right] \tag{A3}$$

Over one complete revolution the average is then

$$\overline{V}(r) = \frac{V^+ + V^-}{2} = V_T\left[1 - \xi\delta_0^2 - \xi(r\cos\beta)^2\right] \tag{A4}$$

Over the complete acceleration life of a particle, the average acceleration voltage will be

$$\overline{E} = \frac{\int_0^{\mathcal{R}} w(r) \times \overline{V}(r)dr}{\int_0^{\mathcal{R}} w(r)dr} \tag{A5}$$

where $\mathcal{R}$ is the extraction radius and $w(r)$ is a weighting function that accounts for the variation of orbit-to-orbit spacing with increasing orbit radius. This variation is such that the number of orbits per unit radius is very nearly proportional to the radius, and so the correct weighting function is just $w(r) = r$.

Carrying out the integration with this weighting function yields

$$\overline{E} = V_T\left\{1 - \xi\left[\delta_0^2 + \frac{(\mathcal{R}\cos\beta)^2}{2}\right]\right\} \tag{A6}$$

When $\overline{\delta}$ is defined as

$$\overline{\delta} = \sqrt{\delta_0^2 + \frac{(\mathcal{R}\cos\beta)^2}{2}}$$

equation (A6) can be written

$$\overline{E} = V_T\left(1 - \xi\overline{\delta}^2\right) = V(\overline{\delta}) \tag{A7}$$

For the Lewis cyclotron, $\delta_0 = 0.699$ meter, $\mathcal{R} = 0.752$ meter, and $\beta = 22.5^{\circ}$. Therefore, at a point δ 0.853 meter from the dee tip, the local dee voltage will be equal to the average accelerating-gap voltage. This point on the dee is indicated in figure 8 (p. 13). In figure 17 the voltage at this point is plotted as a function of the operating frequency.

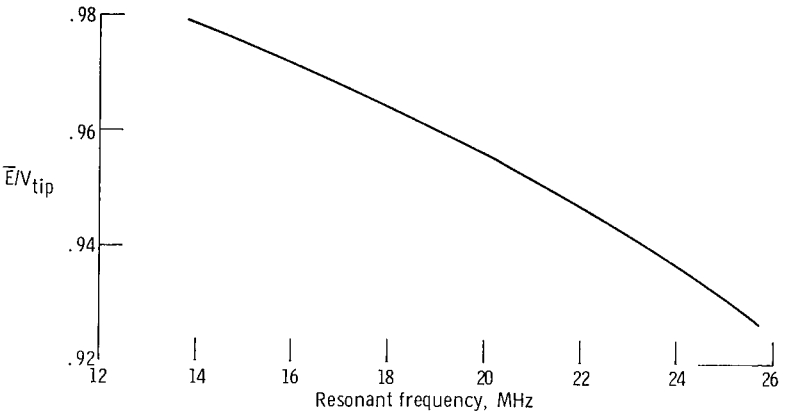

Figure 17. - Frequency variation of average accelerating-gap voltage (normalized to tip voltage, 1.0).

REFERENCES

1. Slater, J. C.: Microwave Transmission. McGraw-Hill Book Co., Inc., 1942.

2. Schlicke, Heinz M.: Essentials of Dielectromagnetic Engineering. John Wiley & Sons, Inc., 1961, p. 39.

NASA-Langley, 1969 —— 24 E-5101

NATIONAL AERONAUTICS AND SPACE ADMINISTRATION
WASHINGTON, D. C. 20546

OFFICIAL BUSINESS

FIRST CLASS MAIL

POSTAGE AND FEES PAID
NATIONAL AERONAUTICS AND
SPACE ADMINISTRATION

"The aeronautical and space activities of the United States shall be conducted so as to contribute . . . to the expansion of human knowledge of phenomena in the atmosphere and space. The Administration shall provide for the widest practicable and appropriate dissemination of information concerning its activities and the results thereof."

— NATIONAL AERONAUTICS AND SPACE ACT OF 1958

NASA SCIENTIFIC AND TECHNICAL PUBLICATIONS

TECHNICAL REPORTS: Scientific and technical information considered important, complete, and a lasting contribution to existing knowledge.

TECHNICAL NOTES: Information less broad in scope but nevertheless of importance as a contribution to existing knowledge.

TECHNICAL MEMORANDUMS: Information receiving limited distribution because of preliminary data, security classification, or other reasons.

CONTRACTOR REPORTS: Scientific and technical information generated under a NASA contract or grant and considered an important contribution to existing knowledge.

TECHNICAL TRANSLATIONS: Information published in a foreign language considered to merit NASA distribution in English.

SPECIAL PUBLICATIONS: Information derived from or of value to NASA activities. Publications include conference proceedings, monographs, data compilations, handbooks, sourcebooks, and special bibliographies.

TECHNOLOGY UTILIZATION PUBLICATIONS: Information on technology used by NASA that may be of particular interest in commercial and other non-aerospace applications. Publications include Tech Briefs, Technology Utilization Reports and Notes, and Technology Surveys.

Details on the availability of these publications may be obtained from:

SCIENTIFIC AND TECHNICAL INFORMATION DIVISION

NATIONAL AERONAUTICS AND SPACE ADMINISTRATION

Washington, D.C. 20546